J|A|C|S
ARTICLES
Published on Web 09/23/2004

Determining the Folding and Unfolding Rate Constants of Nucleic Acids by Biosensor. Application to Telomere G-Quadruplex

Yong Zhao,[†] Zhong-yuan Kan,[†] Zhi-xiong Zeng,[†] Yu-hua Hao,[†] Hua Chen,[‡] and Zheng Tan*[,†,§]

Contribution from the Laboratory of Biochemistry and Biophysics, College of Life Sciences, and College of Mathematics and Statistics, Wuhan University, Wuhan 430072, P. R. China, and Institute of Zoology, Chinese Academy of Sciences, Beijing 100080, P. R. China

Received March 21, 2004; E-mail: tanclswu@public.wh.hb.cn

Abstract: Nucleic acid molecules may fold into secondary structures, and the formation of such structures is involved in many biological processes and technical applications. The folding and unfolding rate constants define the kinetics of conformation interconversion and the stability of these structures and is important in realizing their functions. We developed a method to determine these kinetic parameters using an optical biosensor based on surface plasmon resonance. The folding and unfolding of a nucleic acid is coupled with a hybridization reaction by immobilization of the target nucleic acid on a sensor chip surface and injection of a complementary probe nucleic acid over the sensor chip surface. By monitoring the time course of duplex formation, both the folding and unfolding rate constants for the target−probe duplex can all be derived from the same measurement. We applied this method to determine the folding and unfolding rate constants of the G-quadruplex of human telomere sequence $(TTAGGG)_4$ and its association and dissociation rate constants with the complementary strand $(CCCTAA)_4$. The results show that both the folding and unfolding occur on the time scale of minutes at physiological concentration of K^+. We speculate that this property might be important for telomere elongation. A complete set of the kinetic parameters for both of the structures allows us to study the competition between the formation of the quadruplex and the duplex. Calculations indicate that the formation of both the quadruplex and the duplex is strand concentration-dependent, and the quadruplex can be efficiently formed at low strand concentration. This property may provide the basis for the formation of the quadruplex in vivo in the presence of a complementary strand.

Introduction

Single-stranded nucleic acids, depending on their sequences, can fold into secondary structures via intramolecular interactions. In RNA, secondary structures are a general feature and can be found in many types of RNA molecules.[1] Although genomic DNA is present along with a complementary strand and generally forms a duplex, many sequences that are capable of forming intramolecular structures have been found.[2] For both DNA and RNA, guanine-rich sequences can stack via Hoogsteen hydrogen bonding into a structure referred to as a G-quadruplex (Chart 1a).[3−5] Cytidine-rich sequences can also fold into a structure called an i-motif (Chart 1b) based on intercalated $C-C^+$ base pairing.[6,7] The higher order structures of nucleic acids are essential in many biological processes. For example, specific G-quadruplex structure formed in the c-myc promoter region functions as a transcriptional repressor element.[8] Secondary structures, such as the G-quadruplex, are also believed to be potential therapeutic target for cancer and other diseases.[9−11]

Chart 1. G-Quadruplex (a) and I-Motif (b) Structure Formed by the G-Rich and C-Rich Sequences of Human Telomere DNA

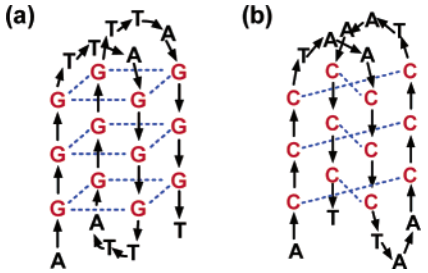

[†] College of Life Sciences, Wuhan University.
[‡] College of Mathematics and Statistics, Wuhan University.
[§] Chinese Academy of Sciences.

(1) Higgs, P. G. *Q. Rev. Biophys.* **2000**, *33*, 199−253.
(2) Catasti, P.; Chen, X.; Mariappan, S. V.; Bradbury, E. M.; Gupta, G. *Genetica* **1999**, *106*, 15−36.
(3) Simonsson, T. *Biol. Chem.* **2001**, *382*, 621−628.
(4) Gilbert, D. E.; Feigon, J. *Curr. Opin. Struct. Biol.* **1999**, *9*, 305−314.
(5) Shafer, R. H.; Smirnov, I. *Biopolymers* **2001**, *56*, 209−227.
(6) Gueron, M.; Leroy, J. L. *Curr. Opin. Struct. Biol.* **2000**, *10*, 326−331.
(7) Snoussi, K.; Nonin-Lecomte, S.; Leroy, J. L. *J. Mol. Biol.* **2001**, *309*, 139−153.
(8) Siddiqui-Jain, A.; Grand, C. L.; Bearss, D. J.; Hurley, L. H. *Proc. Natl. Acad. Sci. U.S.A.* **2002**, *99*, 11593−11598.
(9) Hurley, L. H. *Biochem. Soc. Trans.* **2001**, *29*, 692−696.
(10) Hurley, L. H.; Wheelhouse, R. T.; Sun, D.; Kerwin, S. M.; Salazar, M.; Fedoroff, O. Y.; Han, F. X.; Han, H.; Izbicka, E.; Von Hoff, D. D. *Pharmacol. Ther.* **2000**, *85*, 141−158.
(11) Neidle, S.; Read, M. A. *Biopolymers* **2001**, *56*, 195−208.

The formation of secondary structures also has implications in technical applications that involve nucleic acid hybridization, such as molecular beacon[12] and gene chip analysis.[13] Such analysis is often affected by interference with the secondary structure of the target molecules.[12,14−19]

Besides the secondary structure itself, the kinetics of folding and unfolding is another important factor in the biological functions and therapeutic applications of nucleic acids. The kinetics is quantitatively described by the folding and unfolding rate constants respectively that define not only how fast the structure forms and opens, but also the stability of the structure. Recently, the construction of nanomolecular machinery based on the folding and unfolding of oligonucleotides has been proposed.[20,21] The folding and unfolding rate constants determine how fast such nanomachines can operate. Direct measurement of these two kinetic parameters requires dynamically resolving the different forms of structures. For fast intramolecular conformation interconversions, such measurement is technically difficult. For those sequences in genomes where the DNA strand is present along with a complementary strand, the formation of a secondary structure has to compete with the formation of duplexes. Which form of the structure forms will depend on the relative stability of the two structures.

Among the quadruplex-forming sequences, the G-rich human telomere strand is of special interest because of its involvement in cancer and senescence. Telomeres are the tandem repetitive sequence at the termini of chromosomes. In human cells, telomere consists of tandem repeats of (TTAGGG/CCCTAA) in duplex and carries a single-stranded G-rich 3′ protruding overhang of about 100−300 bases at their ends.[22−24] This telomere overhang serves as a substrate for telomerase and is essential for telomere length homeostasis in telomerase-positive cells, such as germ line and cancer cells. As a guanine-rich repetitive sequence, the G-rich human telomere strand can form intramolecular G-quadruplex structure.[25,26] Folding a single-stranded telomere repeat into a quadruplex prevents it from being elongated by telomerase.[27] Quadruplex-stabilizing molecules have been shown to inhibit telomere elongation by telomerase[28,29] and been explored as potential anti-cancer drugs.[30,31] Telomere overhang can also form another higher structure called a t-loop by invading into the duplex region of the telomere repeat, and such structures may be involved in chromosome end protection and telomere maintenance.[32,33]

In this work, we describe a method that can simultaneously measure both the folding and unfolding rate constants of nucleic acid and its association and dissociation rate constants with the complementary strand using an optical biosensor based on surface plasmon resonance (SPR). We applied this method to determine the four kinetic parameters in the presence of Li^+, Na^+, and K^+ for $(TTAGGG/CCCTAA)_4$ that represents the telomere sequence of human and other vertebrates. The results show that both the unfolded and folded forms of G-rich telomere sequence are short-lived, with half-lives of less than 1 min and a little more than 3 min, respectively, at physiological concentration of K^+. The kinetic parameters allowed us to calculate the formation of different forms of structures when $(TTAGGG)_4$ and $(CCCTAA)_4$ are both present at equilibrium. Although the equilibrium constant was small for the telomere quadruplex and large for the corresponding duplex, which seems to dispute the formation of the quadruplex in the presence of a complementary sequence, it is predicted that the quadruplex structure can be efficiently formed when strand concentration is sufficiently low.

Principle

This section provides only a brief summary of the equations that are used to determine the kinetic parameters. For details of the mathematical derivations and technical issues, see the Supporting Information.

The method is based on a commercial optical biosensor, BIAcore, that employs the surface plasmon resonance (SPR) technique to monitor changes in mass as a result of molecular association and dissociation on a sensor chip surface[34−36] in real time. By immobilizing target molecules on a sensor chip surface and injecting a constant flow of probe molecules over the sensor chip surface (Chart 2a), the association of the probe with the target can be monitored via changes in the refractive index, expressed in response units (RU) in a sensorgram, the value of which is proportional to the quantity of target−probe complex formed (Chart 2b). The theoretical background and basic method for determining the association and dissociation rate constants using the BIAcore system has been described previously.[37,38] A simple target−probe association reaction, such as simple nucleic acid hybridization,[39−41] can be described as

$$R + C \underset{k_d}{\overset{k_a}{\rightleftharpoons}} D \qquad (1)$$

where k_a and k_d are the association and dissociation rate constants, respectively, R is the immobilized target, and C is

(12) Tyagi, S.; Kramer, F. R. *Nat. Biotechnol.* **1996**, *14*, 303−308.
(13) Johnston, M. *Curr. Biol.* **1998**, *8*, R171−R174.
(14) Schwille, P.; Oehlenschlager, F.; Walter, N. G. *Biochemistry* **1996**, *35*, 10182−10193.
(15) Parkhurst, K. M.; Parkhurst, L. J. *Biochemistry* **1995**, *34*, 285−292.
(16) Gamper, H. B.; Cimino, G. D.; Hearst, J. E. *J. Mol. Biol.* **1987**, *197*, 349−362.
(17) Fedorova, O. S.; Podust, L. M.; Maksakova, G. A.; Gorn, V. V.; Knorre, D. G. *FEBS Lett.* **1992**, *302*, 47−50.
(18) Lima, W. F.; Monia, B. P.; Ecker, D. J.; Freier, S. M. *Biochemistry* **1992**, *31*, 12055−12061.
(19) Godard, G.; Francois, J. C.; Duroux, I.; Asseline, U.; Chassignol, M.; Nguyen, T.; Helene, C.; Saison-Behmoaras, T. *Nucleic Acids Res.* **1994**, *22*, 4789−4795.
(20) Alberti, P.; Mergny, J. L. *Proc. Natl. Acad. Sci. U.S.A.* **2003**, *100*, 1569−1573.
(21) Liu, D.; Balasubramanian, S. *Angew. Chem., Int. Ed.* **2003**, *42*, 5734−5736.
(22) Makarov, V. L.; Hirose, Y.; Langmore, J. P. *Cell* **1997**, *88*, 657−666.
(23) Wright, W. E.; Tesmer, V. M.; Huffman, K. E.; Levene, S. D.; Shay, J. W. *Genes Dev.* **1997**, *11*, 2801−2809.
(24) Huffman, K. E.; Levene, S. D.; Tesmer, V. M.; Shay, J. W.; Wright, W. E. *J. Biol. Chem.* **2000**, *275*, 19719−19722.
(25) Wang, Y.; Patel, D. J. *Structure* **1993**, *1*, 263−282.
(26) Parkinson, G. N.; Lee, M. P.; Neidle, S. *Nature* **2002**, *417*, 876−880.
(27) Zahler, A. M.; Williamson, J. R.; Cech, T. R.; Prescott, D. M. *Nature* **1991**, *350*, 718−720.
(28) Teulade-Fichou, M. P.; Carrasco, C.; Guittat, L.; Bailly, C.; Alberti, P.; Mergny, J. L.; David, A.; Lehn, J. M.; Wilson, W. D. *J. Am. Chem. Soc.* **2003**, *125*, 4732−4740.
(29) Mergny, J. L.; Lacroix, L.; Teulade-Fichou, M. P.; Hounsou, C.; Guittat, L.; Hoarau, M.; Arimondo, P. B.; Vigneron, J. P.; Lehn, J. M.; Riou, J. F.; Garestier, T.; Helene, C. *Proc. Natl. Acad. Sci. U.S.A.* **2001**, *98*, 3062−3067.
(30) Kerwin, S. M. *Curr. Pharm. Des.* **2000**, *6*, 441−478.
(31) Neidle, S.; Harrison, R. J.; Reszka, A. P.; Read, M. A. *Pharmacol. Ther.* **2000**, *85*, 133−139.
(32) Greider, C. W. *Cell* **1999**, *97*, 419−422.
(33) Griffith, J. D.; Comeau, L.; Rosenfield, S.; Stansel, R. M.; Bianchi, A.; Moss, H.; de Lange, T. *Cell* **1999**, *97*, 503−514.
(34) Fivash, M.; Towler, E. M.; Fisher, R. J. *Curr. Opin. Biotechnol.* **1998**, *9*, 97−101.
(35) Schuck, P. *Curr. Opin. Biotechnol.* **1997**, *8*, 498−502.
(36) Raghavan, M.; Bjorkman, P. J. *Structure* **1995**, *3*, 331−333.
(37) Karlsson, R.; Michaelsson, A.; Mattsson, L. *J. Immunol. Methods* **1991**, *145*, 229−240.

Chart 2. Schematic Illustration of the BIAcore Optical Detection Device[a]

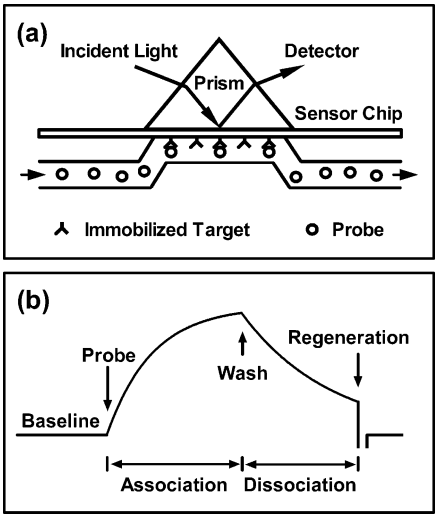

[a] (a) Solution of probe molecules is injected over the sensor chip surface, on which target molecules are immobilized. (b) Binding of probe molecules to target molecules results in an increase in surface mass that is reflected by an increase in response units (RU) in a sensorgram in real time.

the probe that is injected over the sensor chip surface. The formation of target−probe complex D and later the dissociation of bound probe can be quantitated by the SPR signal that satisfies the following equations respectively:

$$U = U_{\max}\frac{k_a C}{k_a C + k_d}[1 - e^{-(k_a C + k_d)t}] \quad (2)$$

$$U = U_w\, e^{-k_d(t - t_w)}, \quad (t \geq t_w) \quad (3)$$

where U_{max} represents the maximum probe binding capacity, U_w the amount of target−probe complex at time t_w when washing is started, and U the amount of target−probe complex at time t, all expressed in response unit (Chart 3b). The k_a and k_d values can be determined by fitting a sensorgram to the above two equations.

Our method for the measurement of the folding and unfolding rate constants of nucleic acids is an expansion of the above simple association−dissociation model where the immobilized target can adopt two different conformational states, only one of which has the ability to associate with the probe (Chart 3a). In the absence of a probe, the conformational interconversion between the two states can be described as

$$Q \underset{k_f}{\overset{k_u}{\rightleftharpoons}} R \quad (4)$$

where Q denotes the folded form of the immobilized target nucleic acid, R is the same target nucleic acid in the linear or relaxed state, and k_f and k_u are the folding and unfolding rate constants, respectively.

When a constant flow of complementary probe nucleic acid is injected over the sensor chip surface, the folding and unfolding reaction of the immobilized nucleic acid is then coupled with a hybridization reaction that can be described as

$$Q \underset{k_f}{\overset{k_u}{\rightleftharpoons}} R \quad (5)$$

$$R + C \underset{k_d}{\overset{k_a}{\rightleftharpoons}} D \quad (6)$$

where C denotes the probe injected that can hybridize with R to form duplex D. The formation of duplex D is transduced into SPR signal (Chart 3b), described by the following equation for the association phase:

$$U = U_0 + U_1\, e^{\lambda_1 t} + U_2\, e^{\lambda_2 t} \quad (7)$$

with

$$U_0 = U_{\max} k_a C \frac{k_u}{k_u k_d + k_f k_d + k_u k_a C} \quad (8)$$

$$U_1 = U_{\max} k_a C \frac{\lambda_1 + k_u}{\lambda_2 - \lambda_1}\left(F_Q \frac{(\lambda_2 + k_u)}{k_f(k_d - k_u)} - \frac{\lambda_2}{k_u k_d + k_f k_d + k_u k_a C}\right) \quad (9)$$

$$U_2 = U_{\max} k_a C \frac{\lambda_2 + k_u}{\lambda_1 - \lambda_2}\left(F_Q \frac{(\lambda_1 + k_u)}{k_f(k_d - k_u)} - \frac{\lambda_1}{k_u k_d + k_f k_d + k_u k_a C}\right) \quad (10)$$

$$\lambda_1 = 0.5\left[-(k_u + k_f + k_a C + k_d) + \sqrt{(k_u + k_f + k_a C + k_d)^2 - 4(k_u k_d + k_f k_d + k_u k_a C)}\right] \quad (11)$$

$$\lambda_2 = 0.5\left[-(k_u + k_f + k_a C + k_d) - \sqrt{(k_u + k_f + k_a C + k_d)^2 - 4(k_u k_d + k_f k_d + k_u k_a C)}\right] \quad (12)$$

where U_{max} is the maximum probe binding capacity in response units (RU), C the concentration of probe that is injected over the sensor chip surface, and F_Q the fraction of immobilized nucleic acid in the folded form at the time of injection of the probe nucleic acid. A measurement is started by a brief pulse of alkaline solution (Chart 3b) that regenerates the chip and denatures the immobilized nucleic acid. A solution of the probe nucleic acid is then injected after equilibrating the sensor chip with running buffer for a defined period. F_Q can be calculated as

$$F_Q = \frac{k_f}{k_u + k_f}[1 - e^{-(k_u + k_f)t_{inj}}] \quad (13)$$

where t_{inj} is the time elapsed between the injection of alkaline solution and probe (Chart 3b). For this coupled hybridization model described by reactions 5 and 6, the kinetic parameters k_f, k_u, k_a, and k_d can be determined by fitting the sensorgram (Chart 3b) to eqs 7 and 3.

Materials and Methods

Oligonucleotides. Biotinylated $(TTAGGG)_4$ and 21-mer TGCGTGGAGCCAGCGAGAGAA were synthesized and HPLC purified by TaKaRa Biotechnology (Dalian, China). The biotin is coupled to the

(38) Myszka, D. G. *Methods Enzymol.* **2000**, *323*, 325−340.
(39) Jensen, K. K.; Orum, H.; Nielsen, P. E.; Norden, B. *Biochemistry* **1997**, *36*, 5072−5077.
(40) Gotoh, M.; Hasegawa, Y.; Shinohara, Y.; Shimizu, M.; Tosu, M. *DNA Res.* **1995**, *2*, 285−293.
(41) Wright Lucas, S.; Harding, M. M. *Anal. Biochem.* **2000**, *282*, 70−79.

Chart 3. Coupling the Folding and Unfolding of Immobilized Target Nucleic Acid with Hybridization Reaction on Sensor Chip Surface[a]

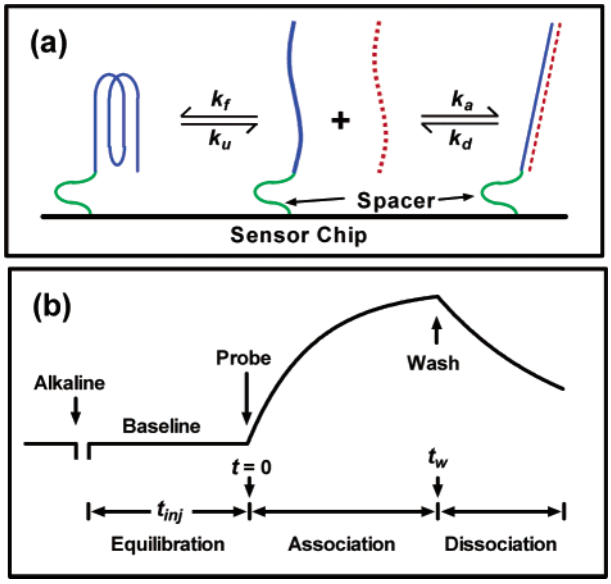

[a] (a) Reactions taking place on the sensor chip surface when the target nucleic acid is immobilized via spacer and the probe nucleic acid passes across the sensor chip surface. (b) Illustrative sensorgram showing different phases of a measurement.

5′ end of the oligonucleotides through a C_{12} spacer. Unlabeled $(TTAGGG)_4$, $(CCCTAA)_4$, and 21-mer TTCTCTCGCTGGCTCCACGCA were purchased from Bochai Biotechnology (Shanghai, China).

UV Melting Profile. The denaturations were carried out on a Beckman DU-640 UV−Vis spectrophotometer equipped with a digital circulating water bath. The absorbance of biotinylated $(TTAGGG)_4$ in 10 mM Tris (pH 7.4), 1 mM EDTA, and 150 mM monovalent cation was monitored at 295 nm[42] while the temperature was increased from 10 to 80 °C at about 0.5−1.5 °C/min. Melting profiles were analyzed by fitting them to a concerted two-state model in which the absorbance A is given by the following equations:[43]

$$A = A_f\theta + A_u(1 - \theta) \quad (14)$$

$$\theta = 1/[1 + e^{(\Delta H^0/R)(1/T - 1/T_m)}] \quad (15)$$

UV Cross-Linking and Gel Mobility Shift Assay. UV cross-linking of $(TTAGGG)_4$ was carried out as described in ref 44. $(TTAGGG)_4$ in TE buffer (pH 7.4) containing 50 mM NaCl was heated at 95 °C for 2 min, and then cooled to 4 °C rapidly and kept at this temperature for 10 min before being irradiated in a CL-1000 ultraviolet cross-linker for 8 min. Irradiated $(TTAGGG)_4$ was separated on 12% denaturing polyacrylamide gel, and the band of cross-linked G-quadruplex was cropped and purified using an E.Z.N.A. poly-gel extraction kit (Omega, Doraville, GA). Un-irradiated $(TTAGGG)_4$ and the purified cross-linked G-quadruplex were 5′-end-labeled with [γ-^{32}P]ATP using T4 polynucleotide kinase (NEB, Hitchin, UK). Oligonucleotide was mixed with *Escherichia coli* single-stranded binding protein in 10 mM Tris (pH 7.4), 1 mM EDTA, and 150 mM LiCl and incubated on ice for 20 min. The oligonucleotide without protein and the oligonucleotide−protein mixture were loaded on 12% native polyacrylamide gel and run with 1× TBE buffer at 10 V/cm for 2 h. The gel was autoradiographed on a Typhoon phosphor imager (Amersham Biosciences, AB, Uppsala, Sweden).

Oligonucleotide Immobilization. Biotinylated oligonucleotide was immobilized on a CM5 sensor chip (BIAcore, Neuchâtel, Switzerland) via streptavidin using a BIAcore X optical biosensor. Streptavidin was coupled to the carboxymethylated dextran matrix covering the surface of the sensor chip using the Amine Coupling Kit (BIAcore) according to manufacturer's instructions. Biotinylated oligonucleotide at 1 μM in coupling buffer (10 mM Tris, pH 7.4, 1 mM EDTA, and 150 mM LiCl) was heated at 95 °C for 5 min and cooled slowly to room temperature, and then injected at a flow rate of 30 μL/min to reach an immobilization of less than 200 RU.

Surface Plasmon Resonance Monitoring of Binding of *E. coli* Single-Stranded DNA Binding Protein to Immobilized Oligonucleotide. The binding of *E. coli* single-strand DNA binding protein to the immobilized oligonucleotides was carried out on a BIAcore X optical biosensor. Protein in running buffer of 10 mM Hepes (pH 7.4), 1 mM EDTA, and 150 mM KCl or LiCl was injected at 30 μL/min, followed by a flow of running buffer. A blank cell was used as reference. The sensor chip was regenerated by injection of 5 μL of 20 mM NaOH.

Measurement of Hybridization Kinetics and Extraction of Kinetic Parameters. Measurements were performed on a BIAcore X optical biosensor. The running buffer contained 10 mM Tris (pH 7.4), 1 mM EDTA, and 150 mM monovalent cation as indicated. For each measurement, 5 μL of 20 mM NaOH was injected at 30 μL/min, followed by 1200 s of running buffer flow. Hybridization was initiated by injecting 45 μL of a complementary oligonucleotide at 30 μL/min, followed by a flow of running buffer at 30 μL/min for 250−300 s. Both the association and dissociation phases were recorded, and a blank cell was used as reference. For each set of kinetic constants under each specified condition, sensorgrams of five injections of complementary oligonucleotide at different concentrations were recorded. The BIAevaluation 3.0 software supplied by the manufacturer of BIAcore provides a convenient interface and an efficient numerical algorithm for fitting sensorgrams to extract kinetic parameters. The software allows the end-user to modify existing models and build new models. Taking advantage of this, we incorporated the coupled hybridization model into the software. Using this model and the built-in simple association and dissociation model, global fitting was carried out to extract k_d using the dissociation phase and then k_f, k_u, k_a (for the hybridization model), or k_a (for the simple hydridization model) using the association phase. Pilot experiments showed that an increase in flow rate of $(CCCTAA)_4$ led to an increase in response signal, indicating that a mass transport effect was present and it was incorporated into the model using the BIAevaluation software.

Results

Formation of Quadruplex Inhibits Oligonucleotide Hybridization. Figure 1 shows the hybridization of $(TTAGGG)_4$ and the 21-mer random oligonucleotide with their complementary strand in Li^+, Na^+, and K^+, respectively. Signal covering both the association and dissociation phases was recorded in real time and expressed as response units, proportional to the duplex formed. The response unit for $(TTAGGG)_4$ obtained in the presence of Na^+ or K^+ was much lower than that in the presence of Li^+, indicating that the hybridization was inhibited in K^+ and Na^+ (Figure 1a). Because the hybridization for the 21-mer oligonucleotide that does not form a secondary structure is not affected by K^+ and Na^+ (Figure 1b), the inhibition of hybridization between $(TTAGGG)_4$ and $(CCCTAA)_4$ can be explained only by the formation of a quadruplex structure. This is in agreement with the UV melting profiles (Figure 2) and the well-known fact that the quadruplex structure forms in K^+ and Na^+ but not in Li^+.[45] The reduced response unit in the

(42) Mergny, J. L.; Phan, A. T.; Lacroix, L. *FEBS Lett.* **1998**, *435*, 74−78.
(43) Germann, M. W.; Kalisch, B. W.; Pon, R. T.; van de Sande, J. H. *Biochemistry* **1990**, *29*, 9426−9432.
(44) Williamson, J. R.; Raghuraman, M. K.; Cech, T. R. *Cell* **1989**, *59*, 871−880.

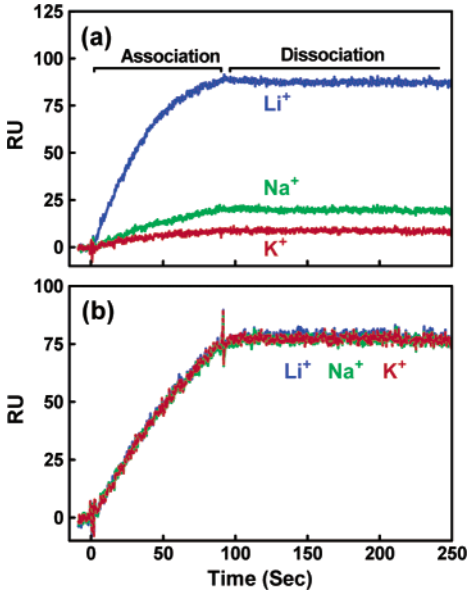

Figure 1. Oligonucleotide hybridization in 150 mM Li^+, Na^+, or K^+ monitored by surface plasmon resonance. (a) $(CCCTAA)_4$ injected at 126 nM against immobilized $(TTAGGG)_4$. (b) TTCTCTCGCTGGCTCCACG-CA injected at 150 nM against immobilized TGCGTGGAGCCAGC-GAGAGAA. The dissociation phase started at 90 s when the mobile phase was switched to running buffer.

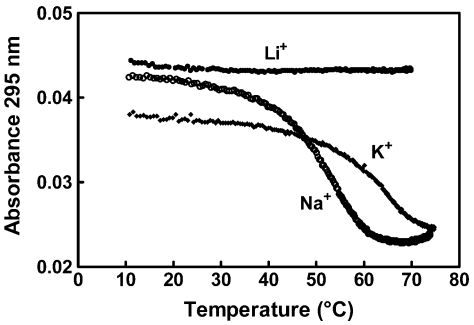

Figure 2. UV-melting profile of biotinylated $(TTAGGG)_4$. Absorbance of oligonucleotide in 150 mM Li^+, Na^+, or K^+ was monitored at 295 nm when the temperature was increased over the range from 10 to 80 °C. The melting temperature (T_m) is estimated to be 52 °C in Na^+ and 64 °C in K^+.

presence of K^+ relative to Na^+ is also in agreement with the fact that K^+ is more effective in stabilizing quadruplex than Na^+ is.[46] The formation of the G-quadruplex structure of the immobilized $(TTAGGG)_4$ in K^+ was also supported by the reduced binding of *E. coli* single-strand DNA binding protein (Figure 3), monitored by surface plasmon resonance. This protein binds single-stranded DNA with high specificity and does not bind to double-stranded DNA.[47] As is shown in Figure 3a, the protein binds to the relaxed $(TTAGGG)_4$ but not the G-quadruplex. The binding of the protein to the immobilized $(TTAGGG)_4$ is greatly reduced in the presence of K^+ compared to Li^+ (Figure 3b), which again can be explained by the formation of the G-quadruplex in K^+ but not in Li^+. It cannot be explained by a direct effect of cation because K^+ slightly elevated the binding of the protein to the immobilized 21-mer oligonucleotide (Figure 3c).

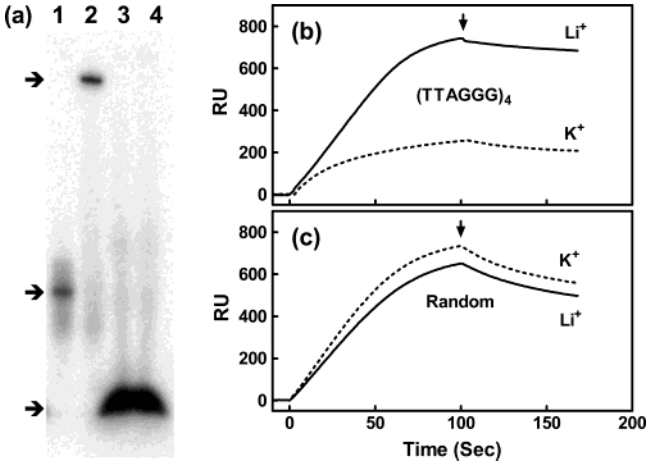

Figure 3. (a) Gel mobility shift assay of the binding of *E. coli* single-stranded DNA binding protein (SSB) to $(TTAGGG)_4$. Lane 1, un-cross-linked $(TTAGGG)_4$ only; lane 2, un-cross-linked $(TTAGGG)_4$ + SSB; lane 3: UV cross-linked $(TTAGGG)_4$ quadruplex only; lane 4, UV cross-linked $(TTAGGG)_4$ quadruplex + SSB. The arrows at the left from top to bottom indicate $(TTAGGG)_4$/SSB complex, free un-cross-linked $(TTAGGG)_4$, and free cross-linked $(TTAGGG)_4$ quadruplex, respectively. The $(TTAGGG)_4$/SSB complex shows a slower migration because of the increased size compared with the free $(TTAGGG)_4$. The cross-linked $(TTAGGG)_4$ quadruplex is more compact and therefore migrates faster than the relaxed form of $(TTAGGG)_4$. (b) Binding of SSB to immobilized $(TTAGGG)_4$ in Li^+ and K^+ monitored by surface plasmon resonance. (c) Binding of SSB to immobilized 21-mer random sequence in Li^+ and K^+ monitored by surface plasmon resonance. Washing started at 100 s (arrows) in both (b) and (c).

Folding and Unfolding Constants of Quadruplex and Association and Dissociation Constants of Duplex. Figures 4 and 5 shows the representative sensorgrams obtained at 25 °C and the theoretical curves obtained by fitting the sensorgrams to both the simple and coupled hybridization models. The sensorgrams obtained in K^+ and Na^+ can be fitted only by the coupled hybridization model (Figure 4a,c) but not by the simple hybridization model (Figure 4b,d), which is an indication of formation of a secondary structure of the immobilized $(TTAGGG)_4$ on the sensor chip surface (see Supporting Information). The sensorgrams obtained in Li^+ can be fitted to both the coupled hybridization model and the simple hybridization model (Figure 5a,b), which is characteristic of the simple hybridization reaction predicted (see Supporting Information). As a control, the sensorgrams of the 21-mer oligonucleotide that does not form a secondary structure can also be fitted by both models (Figure 5c,d), further indicating that the hybridization of $(TTAGGG)_4$ with $(CCCTAA)_4$ in Li^+ is a simple hybridization reaction. As predicted by simulation (see Supporting Information), fitting a simple hybridization reaction to the coupled hybridization model yields a very small k_f relative to k_u. The results shown in Table 1 show that this is also true for real experimental data.

The kinetic parameters obtained from measurements carried out in a 150 mM concentration of cation at either 25 or 37 °C are summarized in Table 2. The stabilization of the quadruplex by the ions, as reflected by the equilibrium constant of quadruplex formation, K_F, is in the order $K^+ > Na^+ \gg Li^+$, which is in agreement with the melting temperature of the human telomere sequence, obtained by UV spectroscopy.[42] The folding rate constant in K^+ is about twice that in Na^+ at both 25 and 37 °C, while the unfolding rate constant in K^+ is 3.5 times smaller at 25 °C and 2.5 times smaller at 37 °C than that

(45) Hardin, C. C.; Perry, A. G.; White, K. *Biopolymers* **2001**, *56*, 147−194.
(46) Balagurumoorthy, P.; Brahmachari, S. K. *J. Biol. Chem.* **1994**, *269*, 21858−21869.
(47) Krauss, G.; Sindermann, H.; Schomburg, U.; Maass, G. *Biochemistry* **1981**, *20*, 5346−5352.

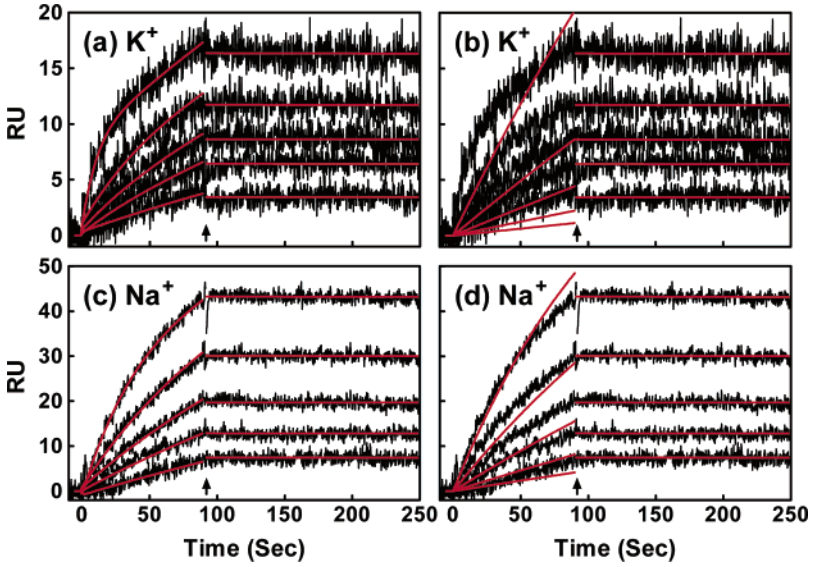

Figure 4. Sensorgrams of the hybridization of immobilized $(TTAGGG)_4$ with $(CCCTAA)_4$ obtained at 25 °C in 150 mM K^+ (a,b) or Na^+ (c,d). $(CCCTAA)_4$ was injected at 4, 8, 16, 32, and 80 nM (a,b) or 4, 8, 16, 32, and 64 nM (c,d). Washing started at 90 s (arrow). Theoretical curves (red) were obtained by fitting the sensorgrams (black) to the coupled hybridization (a,c) or simple hybridization (b,d) model.

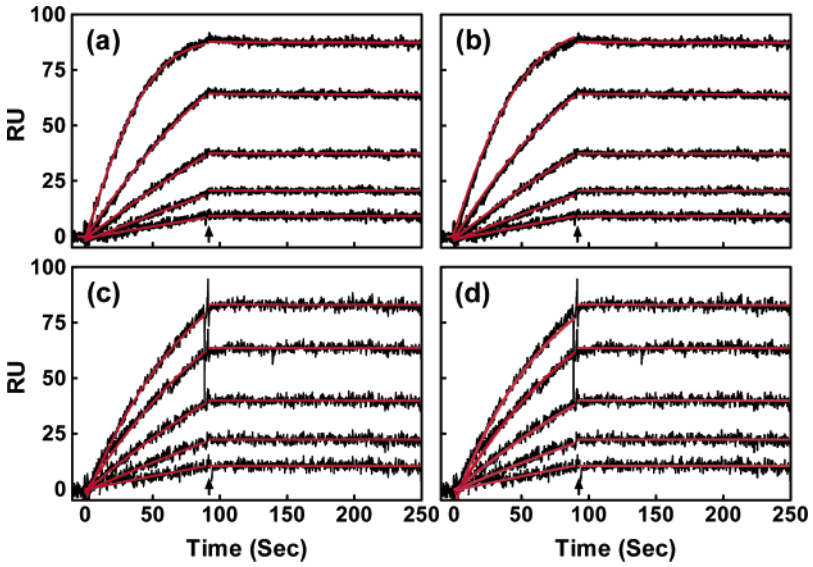

Figure 5. Sensorgrams of the hybridization of immobilized $(TTAGGG)_4$ with $(CCCTAA)_4$ in 150 mM Li^+ (a,b) or of the 21-mer oligonucleotide with its complementary strand in 150 mM Na^+ (c,d), obtained at 25 °C. $(CCCTAA)_4$ was injected at 1, 2, 4, 8, and 16 nM (a,b), and the complementary strand was injected at 12.5, 25, 50, 100, and 150 nM (c,d). Washing started at 90 s (arrow). Theoretical curves (red) were obtained by fitting the sensorgrams (black) to the coupled hybridization (a,c) or simple hybridization (b,d) model.

Table 1. Kinetics Parameters of $(TTAGGG)_4$ in 150 mM Li^+ and the 21-mer 5′-TGCGTGGAGCCAGCGAGAGAA-3′ in 150 mM Na^+ [a]

sequence	fitting model	k_f (s^{-1})	k_u (s^{-1})	k_a (M^{-1} s^{-1})	k_d (s^{-1})
$(TTAGGG)_4$	simple hybridization	n/a	n/a	2.4×10^6 (7.5×10^3)	2.1×10^{-5} (3.1×10^{-6})
	coupled hybridization	8.6×10^{-6} (3.2×10^{-6})	1.9×10^{-2} (9.4×10^{-3})	2.2×10^6 (1.4×10^4)	2.1×10^{-5} (3.1×10^{-6})
21-mer	simple hybridization	n/a	n/a	9.0×10^4 (3.4×10^2)	1.1×10^{-5} (5.2×10^{-6})
	coupled hybridization	1.7×10^{-6} (4.3×10^{-7})	1.9×10^{-3} (3.6×10^{-4})	9.6×10^4 (1.0×10^3)	1.1×10^{-5} (5.2×10^{-6})

[a] Measurements were carried out at 25 °C, and sensorgrams were fitted to both the simple and coupled hybridization models. Numbers in parentheses are standard errors.

in Na^+. Therefore, the better stabilizing effect of K^+ over Na^+ is achieved by increased folding and decreased unfolding of the quadruplex. Changing the temperature from 25 to 37 °C has little effect on the folding rate, but increases the unfolding rate by 3-fold in K^+ and 2-fold in Na^+. This phenomenon is very similar to that observed by Nordgren et al.[48] on the interaction between folded antisense and target RNAs. Over the range from 5 to 37 °C, they found that the association rate constant is relatively independent of temperature, while the dissociation rate constant can vary by several- to 10-fold.

The above measurements were carried out using $(CCCTAA)_4$ in the mobile phase. We also used a shorter complementary strand, i.e., $CCC(AATCCC)_2AAT$, to measure the rate constants. This change is expected to affect k_a and k_d, but not k_f and k_u.

(48) Nordgren, S.; Slagter-Jager, J. G.; Wagner, G. H. *J. Mol. Biol.* **2001**, *310*, 1125−1134.

Table 2. Kinetic Parameters of $(TTAGGG)_4$ Obtained in K^+, Na^+, and Li^+ [a]

	K^+		Na^+		Li^+
	25 °C	37 °C	25 °C	37 °C	25 °C
k_f (s^{-1})	1.2×10^{-2} (8.3×10^{-4})	1.6×10^{-2} (3.7×10^{-4})	7.0×10^{-3} (3.2×10^{-5})	8.2×10^{-3} (6.8×10^{-4})	8.6×10^{-6} (3.2×10^{-6})
k_u (s^{-1})	1.3×10^{-3} (4.7×10^{-5})	3.8×10^{-3} (3.9×10^{-5})	4.6×10^{-3} (1.3×10^{-4})	1.0×10^{-2} (4.1×10^{-4})	1.9×10^{-2} (9.4×10^{-3})
K_F	9.0	4.2	1.5	8.2×10^{-1}	4.5×10^{-4}
$t_{f\,1/2}$ (s)	533	183	151	69	37
$t_{u\,1/2}$ (s)	57.8	43	99	85	8.1×10^4
k_a ($M^{-1}\,s^{-1}$)	1.3×10^6 (7.7×10^4)	6.1×10^5 (8.5×10^3)	6.2×10^5 (7.8×10^3)	7.4×10^5 (2.5×10^4)	2.2×10^6 (1.4×10^4)
k_d (s^{-1})	1.6×10^{-5} (1.2×10^{-5})	6.2×10^{-5} (1.6×10^{-7})	1.2×10^{-5} (6.3×10^{-6})	6.4×10^{-5} (9.7×10^{-6})	2.1×10^{-5} (3.1×10^{-6})
K_A (M^{-1})	7.8×10^{10}	9.8×10^9	5.0×10^{10}	1.2×10^{10}	1.1×10^{11}

[a] Measurements were carried out in a 150 mM concentration of the cation at the temperatures indicated, and sensorgrams were fitted to the coupled hybridization model. K_F is the equilibrium constant for the formation of the telomere quadruplex, given by k_f/k_u, and K_A is the equilibrium constant for the formation of the telomere duplex, given by k_a/k_d. The half-lives, $t_{f\,1/2}$ for the folded form and $t_{u\,1/2}$ for the unfolded form, are calculated using $t_{f\,1/2} = \ln 2/k_u$ and $t_{u\,1/2} = \ln 2/k_f$, respectively. Numbers in parentheses are standard errors.

Table 3. Comparison of Rate Constants Obtained Using Complementary Oligonucleotides of Different Lengths[a]

	K^+		Na^+	
	24-mer	18-mer	24-mer	18-mer
k_f (s^{-1})	1.2×10^{-2} (8.3×10^{-4})	1.1×10^{-2} (9.9×10^{-4})	7.0×10^{-3} (3.2×10^{-5})	7.7×10^{-3} (4.4×10^{-4})
k_u (s^{-1})	1.3×10^{-3} (4.7×10^{-5})	1.6×10^{-3} (7.7×10^{-5})	4.6×10^{-3} (1.3×10^{-4})	4.5×10^{-3} (1.5×10^{-4})
k_a ($M^{-1}\,s^{-1}$)	1.3×10^6 (7.7×10^4)	7.2×10^5 (5.4×10^4)	6.2×10^5 (7.8×10^3)	2.8×10^5 (6.4×10^3)
k_d (s^{-1})	1.6×10^{-5} (1.2×10^{-5})	1.4×10^{-4} (9.5×10^{-6})	1.2×10^{-5} (6.3×10^{-6})	1.6×10^{-4} (3.8×10^{-6})

[a] Measurements were carried out in a 150 mM concentration of the cation at 25 °C using $(AATCCC)_4$ (24-mer) or $CCC(AATCCC)_2AAT$ (18-mer) (as probes), and sensorgrams were fitted to the coupled hybridization model. Numbers in parentheses are standard errors.

Table 4. Comparison of Equilibrium Constants of Duplex and G-quadruplex Obtained from Surface Plasmon Resonance (SPR) and Other Techniques[a]

Duplex

sequence	method	$[Na^+]$ (mM)	T (°C)	ΔG^0 (kcal/mol)	K_A (M^{-1})	ref
$(TTAGGG)_4$	SPR	150	37		1.2×10^{10}	this work
			25		5.0×10^{10}	
$GGG(TTAGGG)_3$	UV melting	100	37	−17	9.7×10^{11}	63
				−18.9	2.1×10^{13}	
$GGG(TTAGGG)_3$	UV melting	100	37	−17	9.7×10^{11}	64
22-mer	microparticles	100	20		$>1 \times 10^{11}$	65

G-Quadruplex

sequence	method	$[Na^+]$ (mM)	T (°C)	ΔG^0 (kcal/mol)	K_F (M^{-1})	ref
$(TTAGGG)_4$	SPR	150	37		8.2×10^{-1}	this work
			25		1.5	
biotin-C_{12}-$(TTAGGG)_4$	UV melting	150	37	−2.08	2.9×10^1	this work
			25	−2.96	1.2×10^2	
$GGG(TTAGGG)_3$	UV melting	100	37	−3	1.3×10^2	42
$(TTAGGG)_4$	CD melting	70	25	−2.5	5.8×10^1	46

[a] Equilibrium constant measured or calculated from ΔG^0 using $\Delta G^0 = -RT \ln(K)$, where ΔG^0 is provided. K denotes either K_A or K_F.

Table 3 shows the results obtained using this 18-mer and their comparison with those obtained using the 24-mer $(CCCTAA)_4$. It can be seen that the k_f or k_u values obtained under both conditions are very close to each other, while the k_a for the 18-mer is reduced roughly by half and k_d increased by 1 order of magnitude compared to the corresponding value for the 24-mer.

Formation of Quadruplex and Duplex at Equilibrium. Except for the 3′ end overhang, the G-rich strand of human telomere is present along with a complementary C-rich strand. In the presence of the complementary strand, whether $(TTAGGG)_4$ forms a quadruplex or duplex will depend on the stability of these two forms of structures, which is quantitatively defined respectively by the equilibrium constants, K_F and K_A. Measurement of the four kinetic parameters allows us to calculate these two constants. A comparison of our data with those available in the literatures is summarized in Table 4. The equilibrium constant obtained on BIAcore for both the G-quadruplex and duplex is smaller by about 2 orders of magnitude than those reported in the other works, indicating that immobilization destabilized both the quadruplex and duplex structures.

With the K_F and K_A, we can assess the competition between quadruplex and duplex formation. We consider a system where both $(TTAGGG)_4$ and $(CCCTAA)_4$ are present. When the folding and unfolding reaction of $(TTAGGG)_4$ and the association between the two oligonucleotides described by reactions 5 and 6 reach equilibrium, we have

$$\frac{Q}{R} = \frac{k_f}{k_u} = K_F \tag{16}$$

$$\frac{D}{RC} = \frac{k_a}{k_d} = K_D \tag{17}$$

Because genomic DNA is present in vivo in a 1:1 ratio with its complementary strand, we consider the situation where the two strands are present at an equimolar ratio. Assuming the total concentration of each strand is C_0, which means

$$R + Q + D = C_0 \tag{18}$$

$$C + D = C_0 \tag{19}$$

then the concentration of $(TTAGGG)_4$ in the quadruplex, duplex, and relaxed forms can be obtained as follows by manipulation of eqs 16−19:

$$Q = \frac{K_F}{2K_A}(\sqrt{1 + 4C_0K_AF_U} - 1) \tag{20}$$

$$D = C_0 - \frac{1}{2K_AF_U}(\sqrt{1 + 4C_0K_AF_U} - 1) \tag{21}$$

$$R = \frac{1}{2K_A}(\sqrt{1 + 4C_0K_AF_U} - 1) \tag{22}$$

where

$$F_U = \frac{k_u}{k_u + k_f}$$

Using eqs 20−22, we calculated the formation of different structures of $(TTAGGG)_4$ in the presence of equimolar $(CCCTAA)_4$ at equilibrium using the kinetic parameters obtained, and the results are presented in Figure 6. The formations of quadruplex and duplex are both dependent on strand concentration. At 10^{-6} M or higher, $(TTAGGG)_4$ mainly exists in the duplex form. As the concentration decreases, the fraction of duplex decreases and that of quadruplex increases. At 10^{-11} M or lower, quadruplex formation approaches its maximum. In K^+, quadruplex can account for more than 80% of the total molecules at 37 °C and more than 90% at 25 °C. Since the quadruplex is less stabilized in Na^+ than in K^+, its content is less than 50% in Na^+ at 37 °C.

Technical Issues Affecting the Quality of Rate Constant Extraction. There are six parameters, namely, k_f, k_u, k_a, k_d, U_{max}, and t_{inj}, involved in defining a sensorgram for a coupled hybridization reaction. By definition, U_{max} and t_{inj} are known constants. U_{max} can be obtained from the net increase in RU after the target oligonucleotide is immobilized or determined directly by injecting the complementary oligonucleotide at saturating concentration under a condition under which the immobilized oligonucleotide does not fold. Although k_f, k_u, k_a, and k_d can all be extracted by fitting the association phase to the coupled hybridization model, our simulations showed that better results could be obtained if k_d was extracted using the dissociation phase and k_f, k_u, and k_a using the association phase. The extraction of k_f, k_u, and k_a by fitting the association phase requires input of three constants, i.e., k_d, U_{max}, and t_{inj}. To investigate how errors in these input constants may affect the determination of the other three constants, fittings were carried out against simulated sensorgrams with the input constants offset from their true values. It was found that k_f, k_u, and k_a could be precisely determined even if k_d had an error as high as 1 order of magnitude. Error in U_{max} had little influence on the determination of k_f and k_a, but did on that of k_u. Therefore, a precise U_{max} is important for the determination of k_u. The effect of error in t_{inj} strongly depends on the status of the immobilized target oligonucleotide. When a probe oligonucleotide was injected during the early stage of equilibration, a small error in timing produced a large error in k_f, k_u, and k_a. However, when the injection was made at a later stage, large errors in timing produced little errors in these parameters. These results recommend injection of the complementary oligonucleotide when the immobilized target oligonucleotide is approaching equilibrium. More details regarding the above issues can be found in the Supporting Information.

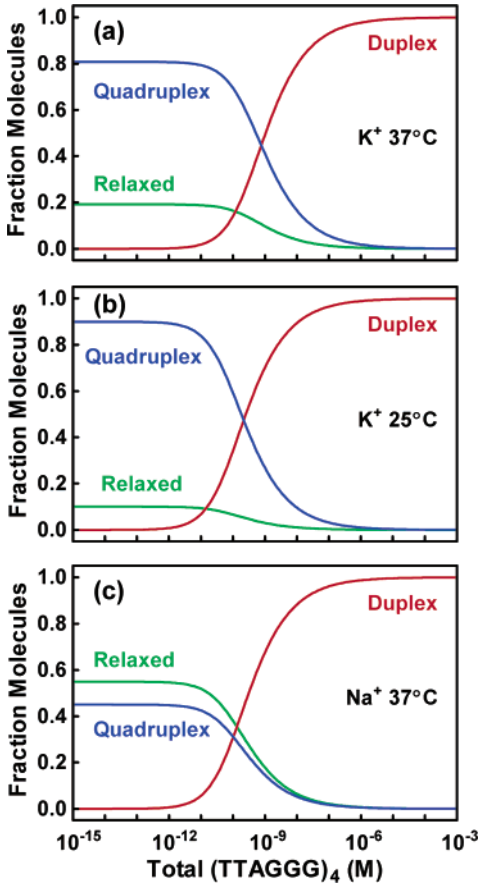

Figure 6. Dependence of quadruplex and duplex formation at equilibrium on strand concentration in a mixture of $(TTAGGG)_4$ and $(CCCTAA)_4$ at equimolar ratio. The quantity of the quadruplex Q, duplex D, or relaxed form R of $(TTAGGG)_4$ was calculated using the k_f, k_u, k_a, and k_d values obtained at (a) 37 °C in 150 mM K^+, (b) 25 °C in 150 mM K^+, and (c) 37 °C in 150 mM Na^+ (Table 2) and expressed as fraction of total molecules.

Discussion

The stability of the quadruplex can be determined from either the thermodynamic properties or the folding and unfolding kinetics. However, kinetic parameters provide additional information about how fast the interconversion between different conformations takes place. There have been many studies on the thermodynamics of quadruplex formation[45] but much less on the kinetics. Recently, the measurement of the unfolding rate of fluorescently labeled human telomere repeats using real-time fluorescence resonance energy transfer (FRET) has been reported by Green et al.[49,50] Compared with their data, the k_u

(49) Green, J. J.; Ying, L.; Klenerman, D.; Balasubramanian, S. *J. Am. Chem. Soc.* **2003**, *125*, 3763−3767.

Table 5. Comparison of Standard Free Energy Change, ΔG^0, of G-Quadruplex Obtained from Surface Plasmon Resonance (SPR) and Denaturation Profile

sequence	method	cation (concn, mM)	ΔG^0(298 K) (kcal/mol)	ΔG^0(310 K) (kcal/mol)	reference
$(TTAGGG)_4$	SPR	Na^+ (150)	−0.24	1.22	this work[a]
		K^+ (150)	−1.30	−0.88	
biotin-C_{12}-$(TTAGGG)_4$	UV melting	Na^+ (150)	−2.96	−2.08	this work[b]
		K^+ (150)	−3.32	−2.30	
$(TTAGGG)_4$	CD melting	Na^+ (70)	−2.5		46
		K^+ (70)	−5.2		
$GGG(TTAGGG)_3$	UV melting	Na^+ (100)		−3.0	42
		K^+ (100)		−5.1	

[a] ΔG^0 was calculated using $\Delta G^0 = -RT \ln(K_F)$. [b] ΔG^0 was calculated using $\Delta G^0 = \Delta H^0(1 - T/T_m)$.

we obtained at 37 °C (1×10^{-2} s^{-1}) in Na^+ is within the same order of magnitude as theirs (6×10^{-3} s^{-1}) obtained under similar conditions. Using the relationship $k_f = k_u K_F$, in which K_F was determined from UV melting data, they estimated the folding constant to be 2.4×10^{-2} s^{-1} at 37 °C in Na^+. This value is also within the same order of magnitude as ours (8.2×10^{-3} s^{-1}) obtained under similar conditions. In an earlier work, the folding and unfolding of a different telomeric sequence, $(T_4G_4)_4$ from *Oxytricha*, were studied in 50 mM K^+ and Na^+ by Raghuraman and Cech.[51] The unfolded DNA was separated from the folded form by hybridization to the complementary sequence $(C_4A_4)_8$ and electrophoresis on gel. These authors reported a k_f of $\geq 2.3 \times 10^{-2}$ s^{-1} in 50 mM K^+ and 1.7×10^{-3} s^{-1} in 50 mM Na^+ respectively at 37 °C. Compared with these two values, our data obtained under similar conditions are all within the same order of magnitude as those of the $(T_4G_4)_4$ from *Oxytricha*. However, the k_u in the work is estimated to be on the order of 10^{-5} s^{-1}, which is 2 orders of magnitude smaller than ours. This difference might be due to differences in the sequence and/or the techniques used.

The work by Green et al.[49] shows that attaching fluorescent dye to each end of $GGG(TTAGGG)_3$ reduced its melting temperature (T_m) by 9 °C for the G-quadruplex, indicating that the structure is destabilized. The molecular weights of the two dyes they used were 792 (Cy5) and 387 (tetramethylrhodamine). Compared to the attachment of fluorescent dye, immobilization of nucleotide to the solid surface is like attaching one end to a molecule of infinite mass. The sensor chip used in our work is coated with a carboxymethylated dextran polymer that tethers off the chip surface. Even though the nucleotide was linked to the polymer through a C_{12} spacer to further reduce steric hindrance, our results indicate that the immobilization of $(TTAGGG)_4$ destabilized the quadruplex structure. The equilibrium constant K_F we obtained in Na^+ is greater than 1 at 25 °C and less than 1 at 37 °C, indicating that the T_m (at which $K_F = 1$) for the immobilized $(TTAGGG)_4$ is between 25 and 37 °C, which is lower than the T_m of 52 °C estimated from the UV melting curve for the same oligonucleotide in solution. A comparison of the standard free energy change, ΔG^0, listed in Table 5 shows that the values obtained for the immobilized $(TTAGGG)_4$ are much higher than those obtained in solution for the same sequence or a sequence that does not carry TTA at the 5′ end. Therefore, the kinetic parameters measured by our method are different from those obtained for oligonucleotide in solution because of the destabilizing effect of immobilization. However, the situation of immobilized $(TTAGGG)_4$ may be closer to the in vivo condition, because the G-rich telomere overhang is attached to the chromosome.

Since our measurements also provide the association and dissociation constants for the telomere duplex, comparing these data with those from other works may also help judge the reliability of our method. The closest situation found in the literature is the work by Gotoh et al.,[40] who measured DNA hybridization in Na^+ at 37 °C using BIAcore, the same instrument we used in this work. For a complementary 20-mer duplex, they obtained a k_a of 2.9×10^5 M^{-1} s^{-1}, which is 1/2.5 of ours (7.4×10^5 M^{-1} s^{-1}), and a k_d of 1.2×10^{-4} M^{-1} s^{-1}, which is two times greater than ours (6.4×10^{-5} s^{-1}). Duplex stability depends on not only base content but also sequence length. Compared with their data, a slightly greater k_a and smaller k_d for our telomere duplex is reasonable since the oligonucleotide we used is 4 bases longer than theirs.

The parameters k_f and k_u provide information about how fast the G-rich telomere strand closes and opens and how these processes are affected by K^+, Na^+, and Li^+. They reveal that the folding and unfolding occur on a time scale of minutes in K^+ and Na^+. In K^+ at 37 °C, the folded form has a half-life of about 3 min and the unfolded form less than 1 min (Table 2). The G-rich telomere overhang serves as a substrate for the telomerase, which adds telomere repeats to the telomere ends and is essential for maintaining telomere length in immortal cells.[52,53] With such a fast unfolding rate, it is clear that the folding of the telomere overhang into the quadruplex per se will not entirely protect it from being elongated by telomerase unless the quadruplex is actively stabilized by other factors. We believe that this property is important for quadruplex-stabilizing molecules to inhibit telomere elongation by telomerase.[30,31] On the other hand, we speculate that this property is also important to make the G-rich telomere strand accessible to and elongated by telomerase. Long-lived quadruplex would prevent telomere from being accessed by telomerase.

Except for the single-stranded overhang, the major part of the G-rich telomere strand is present along with the complementary C-rich strand. The formation of quadruplex structure in this region will have to compete with the formation of duplexes. The four kinetic parameters, k_f, k_u, k_a, and k_d, quantitatively define the stability of and competition between these two structures. Despite the large K_A and small K_F (Table 2), which seems to dispute the formation of quadruplex in the presence of a complementary sequence, our calculations predicts

(50) Ying, L.; Green, J. J.; Li, H.; Klenerman, D.; Balasubramanian, S. *Proc. Natl. Acad. Sci. U.S.A.* **2003**, *100*, 14629−14634.
(51) Raghuraman, M. K.; Cech, T. R. *Nucleic Acids Res.* **1990**, *18*, 4543−4552.
(52) Autexier, C.; Greider, C. W. *Trends Biochem. Sci.* **1996**, *21*, 387−391.
(53) Blasco, M. A. *Eur. J. Cell. Biol.* **2003**, *82*, 441−446.

that the quadruplex might form at low strand concentration. This is not difficult to understand because at low strand concentration, the formation of G-quadruplex will face less competition to form duplex. The intracellular concentration of K^+ is thought to be 100−200 mM.[54] Typical animal cells have a diameter of about 10−30 μm. For a very rough estimation, 92 telomeres in human cells would make a concentration of 3.65×10^{-11} M in a cell, assuming the cell to have a diameter of 20 μm. The results in Figure 6 show that, in physiologically relevant concentrations of K^+, $(TTAGGG)_4$ can readily form a quadruplex at such strand concentration when existing with an equimolar complementary strand. The in vivo situation is certainly much more complicated than simply a matter of concentration. However, the ability for the G-rich strand to form a quadruplex in the presence of a complementary strand at low concentration might provide the basis for the formation of quadruplexes in vivo. The concentration dependence of quadruplex formation also explains some results in published work in which a G-quadruplex is detected or not. In the work by Phan and Mergny,[55] only duplex but no quadruplex was detected by NMR for $AGGG(TTAGGG)_3$ at neutral pH under a strand concentration of 0.1 mM, which, as depicted in our Figure 6, might be too high to permit formation of quadruplex. In another work, by Risitano and Fox,[56] formation of quadruplex by $(TTAGGG)_4$ was detected under a much lower strand concentration at 0.1 μM.

Optical biosensors, such as BIAcore (from BIAcore, Sweden, http://www.biacore.com) and IAsys (Affinity Sensors, UK, http://www.affinity-sensors.com), provide powerful tools for characterizing the kinetic properties of the intermolecular interaction that takes place between molecules.[57] They have been widely used in the characterization of biological macromolecular interactions[58] in general, and in particular in the determination of the association and dissociation constants of antibody−antigen,[59] receptor−ligand,[60] RNA/DNA−protein,[61,62] and DNA hybridization[39−41] reactions. The method we developed expands the application of these biosensors to study the kinetics of intramolecular conformation interconversion. In principle, it is applicable to any molecule that exists in two conformational states, one of which can be bound by a probe. The key in this method is the coupling of the intramolecular conformation interconversion with an intermolecular association reaction. In such system, the association process is then a function of all the kinetic parameters that govern each reaction. By monitoring the time course of intermolecular association in real time, the kinetic parameters for both reactions can be resolved. In the case of nucleic acid, this includes not only the folding and unfolding rate constants for intramolecular structures, but also the association and dissociation rate constants for intermolecular duplexes that are normally difficult to measure because of the interference of intramolecular folding. For those intramolecular conformation interconversions that are fast and take place once the molecules are made in solution, the kinetic parameters may be difficult to obtain by conventional techniques, but can be readily measured by our method. Secondary structure is important in biological process. In genomic DNA, all sequences (except for the single-stranded overhang at the telomere terminus) are present along with their complementary strands; therefore, the formation of a secondary structure has to compete with the formation of a duplex. The interplay of these two processes is quantitatively defined by the four kinetic parameters, k_f, k_u, k_a, and k_d. The capability for our method to simultaneously obtain the four kinetic parameters by a single technique should be especially useful in studying such processes in a quantitative manner. Although the method was developed on BIAcore, it can also be used on similar affinity biosensors, such as the IAsys and other emerging ones, that use surface-immobilized target molecules and in which the concentration of probe molecules in the solution phase can be treated as a constant. Besides the G-quadruplex structure, the folding and unfolding kinetics of the i-motif structure of the C-rich telomere sequence is also being successfully studied in our laboratory.

Acknowledgment. This work was supported by grants nos. 39925008 and 30270314 from NSFC and G2000057001 from MSTC.

Supporting Information Available: Details of mathematical derivations of the equations, numerical simulations and fittings, and technical issues. This material is available free of charge via the Internet at http://pubs.acs.org.

JA048398C

(54) Alberts, B.; Bray, D.; Lewis, J.; Raff, M.; Roberts, K.; Watson, J. D. *Molecular Biology of the Cell*; Garland Publishing: New York, 1983.
(55) Phan, A. T.; Mergny, J. L. *Nucleic Acids Res.* **2002**, *30*, 4618−4625.
(56) Risitano, A.; Fox, K. R. *Biochemistry* **2003**, *42*, 6507−6513.
(57) Rich, R. L.; Myszka, D. G. *Curr. Opin. Biotechnol.* **2000**, *11*, 54−61.
(58) Wilson, W. D. *Science* **2002**, *295*, 2103−2105.
(59) Altschuh, D.; Dubs, M. C.; Weiss, E.; Zeder-Lutz, G.; Van Regenmortel, M. H. *Biochemistry* **1992**, *31*, 6298−6304.
(60) Rich, R. L.; Hoth, L. R.; Geoghegan, K. F.; Brown, T. A.; LeMotte, P. K.; Simons, S. P.; Hensley, P.; Myszka, D. G. *Proc. Natl. Acad. Sci. U.S.A.* **2002**, *99*, 8562−8567.
(61) Katsamba, P. S.; Park, S.; Laird-Offringa, I. A. *Methods* **2002**, *26*, 95−104.
(62) Conway de Macario, E.; Rudofsky, U. H.; Macario, A. J. *Biochem. Biophys. Res. Commun.* **2002**, *298*, 625−631.
(63) Li, W.; Miyoshi, D.; Nakano, S.; Sugimoto, N. *Biochemistry* **2003**, *42*, 11736−11744.
(64) Li, W.; Wu, P.; Ohmichi, T.; Sugimoto, N. *FEBS Lett.* **2002**, *526*, 77−81.
(65) Wilkins Stevens, P.; Henry, M. R.; Kelso, D. M. *Nucleic Acids Res.* **1999**, *27*, 1719−1727.